

# Scalable Purification of Adeno-Associated Virus Serotype 1 (AAV1) and AAV8 Vectors, Using Dual Ion-Exchange Adsorptive Membranes

Takashi Okada,<sup>1,2</sup> Mutsuko Nonaka-Sarukawa,<sup>2</sup> Ryosuke Uchibori,<sup>2</sup> Kazue Kinoshita,<sup>1</sup> Hiromi Hayashita-Kinoh,<sup>1</sup> Yuko Nitahara-Kasahara,<sup>1</sup> Shin'ichi Takeda,<sup>1</sup> and Kei-ya Ozawa<sup>2</sup>

## Abstract

*In vivo* gene transduction with adeno-associated virus (AAV)-based vectors depends on laborious procedures for the production of high-titer vector stocks. Purification steps for efficient clearance of impurities such as host cell proteins and empty vector particles are required to meet end-product specifications. Therefore, the development of alternative, realistic methods to facilitate a scalable virus recovery procedure is critical to promote *in vivo* investigations. However, the conventional purification procedure with resin-based packed-bed chromatography suffers from a number of limitations, including variations in pressure, slow pore diffusion, and large bed volumes. Here we have employed disposable high-performance anion- and cation-exchange membrane adsorbers to effectively purify recombinant viruses. As a result of isoelectric focusing analysis, the isoelectric point of empty particles was found to be significantly higher than that of packaged virions. Therefore, AAV vector purification with the membrane adsorbers was successful and allowed higher levels of gene transfer *in vivo* without remarkable signs of toxicity or inflammation. Electron microscopy of the AAV vector stocks obtained revealed highly purified virions with as few as 0.8% empty particles. Furthermore, the membrane adsorbers enabled recovery of AAV vectors in the transduced culture supernatant. Also, the ion-exchange enrichment of retroviral vectors bearing the amphotropic envelope was successful. This rapid and scalable viral purification protocol using disposable membrane adsorbers is particularly promising for *in vivo* experimentation and clinical investigations.

## Introduction

ADENO-ASSOCIATED VIRUS (AAV) and retroviral vectors are commonly used for gene transduction experiments. With the increasing utility of recombinant AAV (rAAV) or retrovirus as a gene therapy vector, routine production and purification of large amounts of highly purified vector particles for preclinical studies are prerequisite to future clinical investigations. However, the production and purification of recombinant virus stocks by current techniques entail cumbersome procedures not suited to the clinical setting.

In most situations, large-scale propagation of recombinant AAV uses transduction of HEK-293 cells and follows a streamlined concept of cell harvest, purification through CsCl density centrifugation, and concentration of the viral particle fraction. Conventionally, rAAV particles have been purified by rounds of isopycnic banding in CsCl density gradients (Merten *et al.*, 2005). This method of purification is

inconvenient because the development of the linear gradient takes greater than 24 hr per round in a standard ultracentrifuge. Consequently, the method of purification based on rounds of CsCl density centrifugation is not scalable and yields product of insufficient purity and transduction potency (Gao *et al.*, 2000). Therefore, an alternative scalable purification procedure that is able to clear impurities including host cell proteins and empty particles is needed to meet end-product specifications.

Defined serum-free conditions have great conceptual advantages for biological safety and standardization of the production of clinical gene transfer vectors (Glimm *et al.*, 1998). Although a conventional protocol to concentrate the retroviral vector can provide a high-titer stock (Tamura *et al.*, 2001), accomplishment of the serum-free conditions has not yet been established. In addition, unlike the pseudotyped retroviral vectors bearing the vesicular stomatitis virus glycoprotein G (VSV-G), retroviral vectors bearing the amphotropic

<sup>1</sup>Department of Molecular Therapy, National Institute of Neuroscience, National Center of Neurology and Psychiatry, Tokyo, Japan 187-8502.

<sup>2</sup>Division of Genetic Therapeutics, Center for Molecular Medicine, Jichi Medical University, Tochigi, Japan 329-0498.

envelope protein cannot withstand the shearing forces imposed by ultracentrifugation. Efficient transduction with a high-titer serum-free vector stock can be realized only by using chromatographic approaches, making the virus-based vectors ideally suited for applications in clinical gene therapy.

Chromatography is widely used in the downstream purification steps of vector production (Sommer *et al.*, 2003). However, the resin-based, packed-bed chromatography suffers from a number of limitations in practice. These are associated with pressure drops across the bed, slow pore diffusion, long cycle times, and difficulties in scaling up purification procedures (Knudsen *et al.*, 2001). In this study, we have sought to develop an effective and convenient alternative for the removal of empty viral particles and enrichment of viral vector particles. We have adapted dual ion-exchange membrane chromatography to eliminate empty particles from cleared lysates containing recombinant viruses, using disposable ion-exchange membrane adsorbers. Although a previous report suggested the utility of the membrane-based technology in small-scale work (Duffy *et al.*, 2005), scalable production as well as high-grade purification for *in vivo* experimentation were not distinctly demonstrated. In combination with our large-scale transduction technique using active gassing (Okada *et al.*, 2005), we now have at hand a simple and highly efficient system to produce purified vector stocks. Furthermore, the membrane adsorbers enable effective recovery of the AAV vector in the supernatant of the transduced cell culture. Here, we present a high-throughput method for scalable purification of recombinant AAV or retrovirus, using disposable membrane adsorbers to establish a labor- and cost-effective purification system.

## Materials and Methods

### Cell culture

Propagation of vectors was based on transfection of human embryonic kidney-derived 293 (HEK-293) cells using a 10-tray cell factory (CF10; Nalge Nunc International, Rochester, NY) with a surface area of 6320 cm<sup>2</sup> associated with an active gassing system, as described previously (Okada *et al.*, 2005). Briefly, cells were cultured in Dulbecco's modified Eagle's medium and nutrient mixture F-12 (D-MEM/F-12; Invitrogen, Grand Island, NY) with 10% fetal bovine serum (Sigma-Aldrich, St. Louis, MO), penicillin (100 units/ml), and streptomycin (100 µg/ml) at 37°C in a 5% CO<sub>2</sub> incubator. First, cells were plated at 6.5 × 10<sup>7</sup> cells per CF10 to achieve a monolayer of 20 to 40% confluency when cells initially attached to surface of the flask. The volume of medium used per flask was 1120 ml. Subsequently, cells were grown for 48–72 hr until reaching 70–90% confluence and were then transfected with appropriate plasmids. An aquarium pump (Nisso, Tokyo, Japan) was used to circulate the air through the CF10 with 5% CO<sub>2</sub> with humidity in an incubator.

Canine skeletal myoblasts were isolated from a neonatal Beagle dog. Two grams of hind limb muscle was minced and dissociated with intermittent trituration to make a fine slurry. The mixture was filtrated with a BD Falcon cell strainer (100 µm; BD Biosciences, San Jose, CA) and was collected by centrifugation at 800 × g for 5 min. The cell pellet was resuspended with F-10 medium (Invitrogen) with 20% fetal calf serum (Sigma-Aldrich) and cultured on a collagen

I-coated dish at 37°C in a 5% CO<sub>2</sub> incubator. Three rounds of replating were applied to diminish fibroblasts.

### Construction and propagation of AAV vectors

A proviral plasmid harboring the *EGFP* gene (pAAV-EGFP) under the control of the CAG promoter, a modified chicken β-actin promoter with cytomegalovirus immediate-early (CMV-IE) enhancer, has been described previously (Okada *et al.*, 2005). The rat interleukin (IL)-10 cDNA fragment was inserted into the *EcoRI* site of p3.3CAG-WPRE, which contains the CAG promoter and woodchuck post-transcriptional regulatory element (WPRE). The entire expression cassette was inserted between the AAV2-derived inverted terminal repeats (ITRs) in a pUC-based proviral plasmid, pAAVLacZ, to obtain pAAV1-IL-10.

Half the medium in the CF10 tissue culture flask was exchanged with fresh D-MEM/F-12 containing 10% fetal bovine serum (FBS), 1 hr before transfection of HEK-293 cells. Subsequently, the cells were cotransfected with 650 µg of each plasmid: proviral vector plasmid pAAV-EGFP, AAV-1 chimeric helper plasmid or AAV-8 chimeric helper plasmid, as well as adenoviral helper plasmid pAdeno, using calcium phosphate coprecipitation. Each plasmid was added to 112 ml of 300 mM CaCl<sub>2</sub>. This solution was gently added to the same volume of 2 × HBS (290 mM NaCl, 50 mM HEPES buffer, 1.5 mM Na<sub>2</sub>HPO<sub>4</sub>; pH 7.0) and gently inverted three times to form a uniform solution. This solution was immediately mixed with fresh D-MEM/F-12 containing 10% FBS to produce a homogeneous plasmid solution mixture. Subsequently, the medium in the culture flask was replaced with this plasmid solution mixture. At the end of a 6-hr incubation, the plasmid solution mixture in the culture flask was replaced with prewarmed fresh D-MEM/F-12 containing 2% FBS. Cell suspensions were collected 72 hr after transfection and centrifuged at 300 × g for 10 min. Cell pellets were resuspended in 30 ml of Tris-buffered saline (TBS: 100 mM Tris-HCl [pH 8.0], 150 mM NaCl). Recombinant AAV was harvested by five cycles of freeze–thawing of the resuspended pellet. The crude viral lysate was initially concentrated by a brief two-tier CsCl gradient centrifugation for 3 hr (Okada *et al.*, 2002) and then the vector fraction was dialyzed in MHA buffer (3.3 mM morpholinoethanesulfonic acid [MES], 3.3 mM HEPES [pH 6.5, 7.0, 7.5, or 8.0], 3.3 mM sodium acetate).

In parallel with processing the cell pellets, the culture supernatant sample was also processed for the dual ion-exchange procedure by centrifugation and filtration. The culture supernatant fluid, 72 hr after transduction, was sampled and clarified with an appropriate amount of activated charcoal (Wako Pure Chemical Industries, Osaka, Japan). Insoluble debris was removed by centrifugation at 3000 × g for 15 min and filtration. The elucidated culture supernatant was desalted as well as enriched with a hollow fiber cross-flow membrane (100,000 nominal molecular weight cutoff [NMWC]; GE Healthcare, Piscataway, NJ). The sample was concentrated by a brief two-tier CsCl gradient centrifugation for 3 hr and then the vector fraction was dialyzed in MHA buffer.

### Construction and propagation of retroviral vectors

Luciferase cDNA was cloned from the pGL3-Basic vector (Promega, Madison, WI), and inserted into pGCDNsp

(Suzuki *et al.*, 2002) to obtain pDNLuc. To generate a retroviral vector bearing the amphotropic envelope protein or a VSV-G-pseudotyped retroviral vector on a large scale, HEK-293 cells were transduced with 650  $\mu\text{g}$  of pDNLuc, 325  $\mu\text{g}$  of pGag-pol (Ory *et al.*, 1996), and 325  $\mu\text{g}$  of pEnv (Okada *et al.*, 2004) or pVSV-G (Ory *et al.*, 1996) in the CF10 culture flask. Culture supernatant was collected 48 hr after transduction and centrifuged at 300 $\times g$  for 3 min to remove cell debris. To enrich the recombinant retrovirus, vector-containing supernatant was centrifuged at 50,000 $\times g$  for 2 hr or at 6,000 $\times g$  for 16 hr at 4°C. Alternatively, the vector was concentrated and purified by ion-exchange chromatography.

#### Dual ion-exchange chromatography

Chromatography was performed with an ÄKTAexplorer 10S fast protein liquid chromatography (FPLC) system (GE Healthcare Life Sciences) equipped with a 50-ml Superloop (GE Healthcare Life Sciences). A dialyzed vector-containing fraction was loaded onto a cation-exchange membrane with a column volume of 0.18 ml (Acrodisc unit with Mustang S membrane; Pall, East Hills, NY) equilibrated with MHA buffer. After loading at a rate of 3 ml/min, the membrane was washed with 10 column volumes of MHA buffer. Bound samples on the Mustang S membrane was eluted over a 50-column volume span with a 0–2 M linear NaCl gradient in MHA buffer and 1-ml fractions were collected. The eluted sample from the Mustang S membrane was concentrated with a Macrosep 100K Omega filter (Pall) and used for electron microscopic assessment.

The flow-through sample that passed through the Mustang S membrane was diluted with 10 volumes of MHA buffer and further loaded at a rate of 3 ml/min onto an anion-exchange membrane with a bed volume of 0.18 ml (Acrodisc unit with Mustang Q membrane; Pall) equilibrated with MHA buffer. The membrane was then washed with 10 column volumes of MHA buffer. Bound virus on the Mustang Q membrane was eluted over a 50-column volume span with a 0–2 M linear NaCl gradient in MHA buffer and 1-ml fractions were collected. Recombinant rAAV particle number was determined by quantitative polymerase chain reaction (Q-PCR) of DNase I-treated stocks with plasmid standards.

#### Sodium dodecyl sulfate–polyacrylamide gel electrophoresis and staining

A peak vector-containing fraction from the anion-exchange membrane (typically fraction 3) was desalted with a Macrosep 100K Omega filter and separated in 0.9-mm-thick 4–20% gradient polyacrylamide gels (Daiichi Pure Chemicals, Tokyo, Japan) with a sodium dodecyl sulfate (SDS) running buffer. Negative staining of the gel was performed with a Snow White kit (Mo Bi Tec, Göttingen, Germany) as per the manufacturer's instructions. Purity of viral band (VP1, VP2, and VP3) was analyzed with NIH Image (version 1.63) software.

#### Electron microscopy

Samples (10  $\mu\text{l}$ ) were spotted onto a carbon-stabilized copper specimen grid and incubated for 1 min. Excess sample was removed with a small piece of filter paper. The samples were then negatively stained for 1 min with 1%

uranyl acetate solution. After removal of excess uranyl acetate, the air-dried grids were viewed with a JEM 2000EX transmission electron microscope (JEOL, Tokyo, Japan) at an accelerating voltage of 100 kV.

#### Isoelectric focusing

Isoelectric focusing (IEF) is an electrophoresis molecular diagnostic operation that separates protein in a pH gradient according to their isoelectric points (*pI*). Samples containing empty particles as well as fully packaged virions certified by electron microscopy were desalted with Amicon-30 (Millipore, Billerica, MA), and evaluated by IEF. Small-format Novex pH 3–10 IEF gels (EC6655A; Invitrogen, Carlsbad, CA) were used in a Novex XCell SureLock mini-cell (Invitrogen) to separate samples and Serva IEF protein markers 3–10 (39212-01; Invitrogen) as per the manufacturer's instructions.

#### Transduction experiments

To confirm transgene expression by the propagated vector *in vivo*, 3-week-old male Wistar rats were injected via the anterior tibial muscle with either CsCl-purified vectors (control,  $n = 12$ ) or ion-exchange membrane-purified AAV1-IL-10 (CsCl + Mustang S/Q [MtgS/Q],  $n = 8$ ) at  $6 \times 10^{10}$  genome copies per animal. Eight weeks after injection, serum IL-10 concentration was estimated by enzyme-linked immunosorbent assay (ELISA) (GE Healthcare Life Sciences; R&D Systems, Minneapolis, MN). Histological analysis of the muscle injection site was performed to examine the tissue for signs of toxicity or inflammation. To analyze the indication in muscle, which is susceptible to virus-mediated inflammation, we used *mdx* mice, a mouse model of Duchenne muscular dystrophy (DMD). Dystrophic muscles injected with the AAV vector reveal drastic immune response, which might be associated with the dystrophin-deficient sarcolemma of muscle fibers (Yuasa *et al.*, 2002). To avoid the effect of transgene, viruses were inactivated by ultraviolet irradiation for 30 min before injection. Male *mdx* mice were injected with either PBS, CsCl-purified particles, or ion-exchange membrane-purified particles of AAV1-IL-10 at  $1 \times 10^{11}$  genome copies per animal via the tibialis anterior muscle at 2 weeks old ( $n = 2$ , each), when the pathology is indistinct. Two weeks after injection, the mice were killed and muscle samples were stained with hematoxylin and eosin (H&E) to analyze the pathology.

Canine myoblasts were transduced with rAAV-EGFP at  $1 \times 10^5$  or  $3 \times 10^5$  genome copies per cell to observe transgene expression under a fluorescence microscope (IX-70; Olympus, Tokyo, Japan) 3 days after infection. U251MG human glioma cells were transduced with luciferase-expressing recombinant retroviruses to evaluate the effect of the various purification procedures. At 96 hr after transduction, luciferase expression in the cells was analyzed with the Bright-Glo luciferase assay system (Promega).

## Results

### Effect of pH on rAAV recovery

The ion-exchange procedure as a downstream purification was compatible with the initial CsCl density centrifugation when vector-containing fractions were desalted by dialysis.

TABLE 1. EFFECT OF pH ON RECOMBINANT ADENO-ASSOCIATED VIRUS SEROTYPE 1 RECOVERY, USING ION-EXCHANGE MEMBRANES

pH	Particles loaded ( $\times 10^{11}$ GC)	Mustang S (cation exchange)		Mustang Q (anion exchange)	
		Particles recovered ( $\times 10^{11}$ GC)	Recovery rate (%)	Particles recovered <sup>a</sup> ( $\times 10^{11}$ GC)	Recovery rate (%)
6.5	35	18	52	8.7	25
7.0	31	5.2	17	13	42
7.5	34	3.4	10	31	90
8.0	39	5	13	34	86

Abbreviation: GC, genome copies.

<sup>a</sup>Particles in the flow-through sample from the cation-exchange procedure were bound and eluted during anion exchange.

rAAV type 1 (rAAV-1) was successfully recovered by ion-exchange chromatography and pH was an effective parameter to control viral particle affinity for the membrane (Table 1). Optimal recovery of vector genomes by the cation-exchange procedure was achieved at pH 6.5, whereas favorable recovery by the anion-exchange procedure was observed at pH 7.5–8.0.

#### Characterization of rAAV purified by dual ion-exchange chromatography

rAAV-1-containing samples collected by a quick two-tier CsCl gradient centrifugation were dialyzed and applied to a cation-exchange membrane, to capture the impurities including particles. Figure 1a demonstrates the chromatogram of the cation-exchange procedure. Subsequently, the unbound flow-through sample in the cation-exchange procedure was

applied to an anion-exchange membrane. The chromatogram in Fig. 1b demonstrates the resolution and dynamic binding capacity of the anion-exchange membrane. The eluted samples were desalted and concentrated by ultrafiltration. Elution profiles of the samples were stably maintained over the repeated purification procedures, although the fraction number of the vector-containing sample can be altered when the elution speed or gradient conditions are modified.

Electron microscopic analysis of the samples collected from the two-tier CsCl centrifugation revealed virions with more than 6% empty particles (Fig. 2a; 91 empty particles out of 1350 virion particles, 6.7%). Interestingly, analysis of the sample eluted from the cation-exchange membrane revealed that the vast majority of the sample was empty particles (Fig. 2b; 694 of 713 particles, 97.3%). On the other hand, the unbound flow-through sample in the cation-exchange procedure

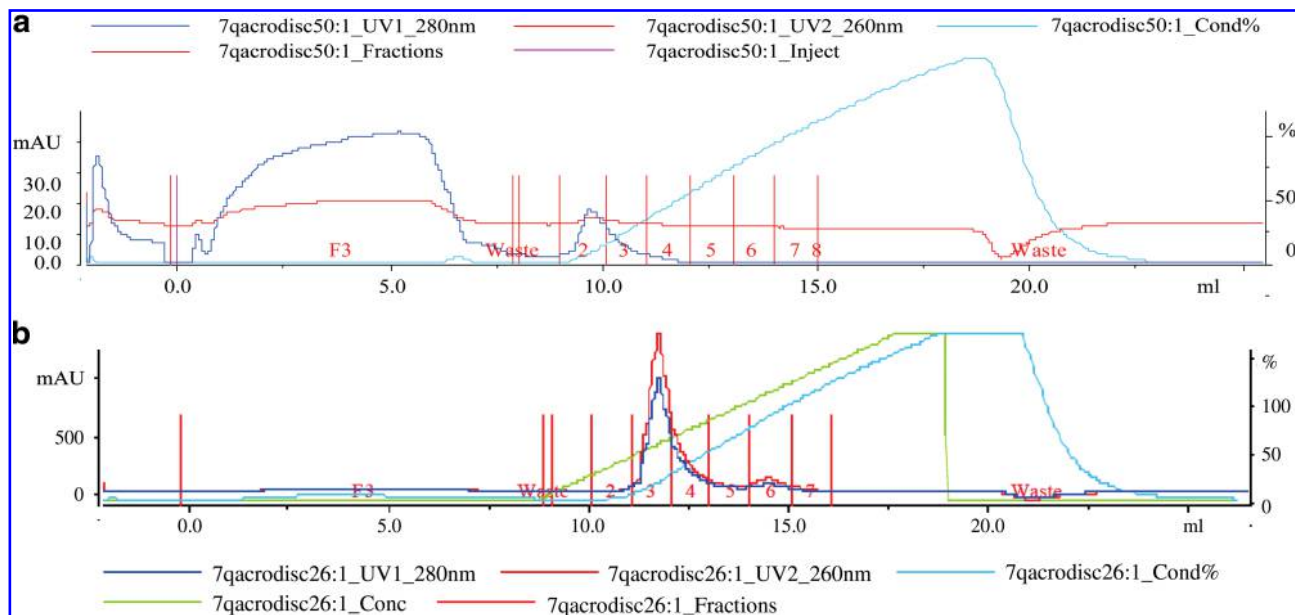
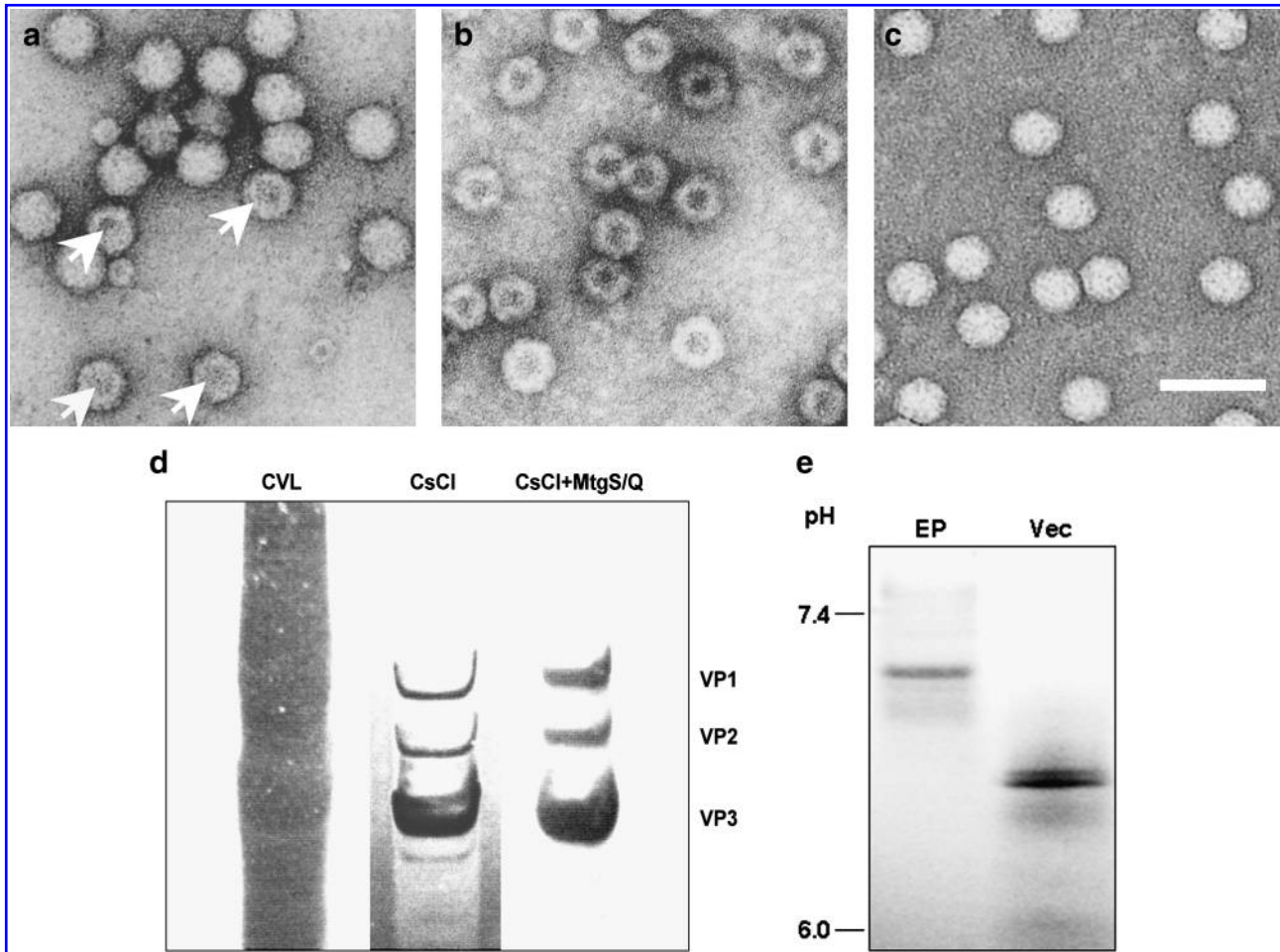


FIG. 1. Elution profile of rAAV-1, using the dual ion-exchange method. (a) Virus-containing dialyzed samples of rAAV-1 enriched by CsCl density centrifugation were pumped through a cation-exchange membrane and analyzed. (b) Subsequently, the flow-through sample was pumped through an anion-exchange membrane. The graph demonstrates the resolution and binding capacity of the 25-mm Acrodisc unit with an ion-exchange membrane at pH 8.0. The chromatography conditions were as follows: loading and wash buffer, 3.3 mM MES, 3.3 mM HEPES, 3.3 mM sodium acetate; elution buffer, 0 to 2 M NaCl gradient in loading buffer in 50 column volumes; and flow rate, 3 ml/min. Red line, OD<sub>260</sub> (mAU); blue line, OD<sub>280</sub> (mAU); green line, salt concentration (%); light blue line, percent conductivity (%).



**FIG. 2.** Electron microscopic assessment of empty particle contamination by dual ion-exchange chromatography. (a) rAAV-1 sample semipurified by two-tier CsCl density centrifugation. Arrows show empty particles (91 empty particles of 1350 virion particles; 6.7%). (b) rAAV-1 sample captured by a cation-exchange membrane. The partially purified sample from (a) was desalted and passed through a cation-exchange membrane to remove cellular proteins and empty particles. A sample enriched in empty particles (694 of 713 particles; 97.3%) was eluted from the cation-exchange membrane with sodium chloride. (c) The flow-through sample was sequentially applied to an anion-exchange membrane to capture the vector particles. Viral particles were eluted with increasing concentrations of sodium chloride, desalted, and concentrated by ultrafiltration. Electron microscopy of the resultant purified stocks revealed virions with less than 1% empty particles (26 of 3365 particles). Scale bar, 50 nm. (d) When the crude viral lysate (CVL) was purified with ion-exchange adsorptive membranes (Mustang S/Q [MtgS/Q]) after the brief two-tier CsCl centrifugation, vector stocks with greater than 90% purity were produced, as indicated by SDS-PAGE analysis. (e) Samples consisting of empty particles (EP) as well as packaged vector virions (Vec) were desalted and evaluated by isoelectric focusing (IEF). Small-format Novex pH 3–10 IEF gels were used to separate samples and Serva IEF protein markers 3–10.

was sequentially applied to an anion-exchange procedure, as dual ion-exchange purification. The samples obtained after the dual ion-exchange purification revealed highly purified virions with as few as 0.8% empty particles (Fig. 2c; 26 of 3365 particles). The analysis was repeated with similar results.

When the viral lysate was purified using dual ion-exchange adsorptive membranes after CsCl centrifugation, vector stocks with greater than 90% purity, as judged by SDS-PAGE analysis, were produced (Fig. 2d).

To estimate the difference in net charge of empty particles and packaged virions, IEF was performed. As the samples move through the gradient, they encounter a point where the pH is equal to their *pI* and they stop migrating. The *pI* of the empty particles was significantly higher than that of packaged virions (Fig. 2e).

#### Effect of purification on transduction efficiency

To confirm transgene expression by the propagated vector *in vivo*, 3-week-old male Wistar rats were injected via the anterior tibial muscle with either CsCl-purified vectors ( $n = 12$ ) or ion-exchange membrane-purified AAV1-IL-10 ( $n = 8$ ) at  $6 \times 10^{10}$  genome copies per animal. Serum IL-10 concentrations in animals transduced with the ion-exchange membrane-purified vectors were significantly higher than in the controls transduced with CsCl-purified vectors ( $519 \pm 261$  vs.  $148 \pm 83$  pg/ml;  $p < 0.001$ ) (Fig. 3a).

Injection of the ion-exchange membrane-purified vector particles into dystrophic muscles verified minimal inflammation. To analyze the effect on the histology of the tissue that is susceptible to virus-mediated inflammation, we used *mdx*

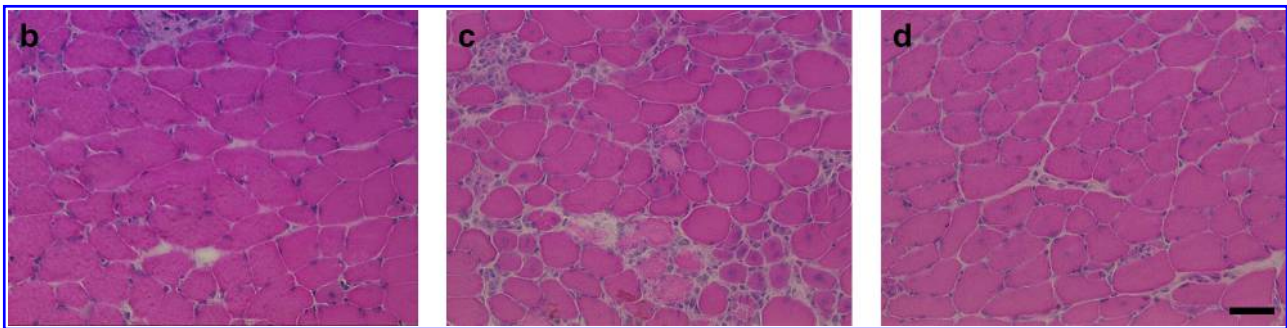
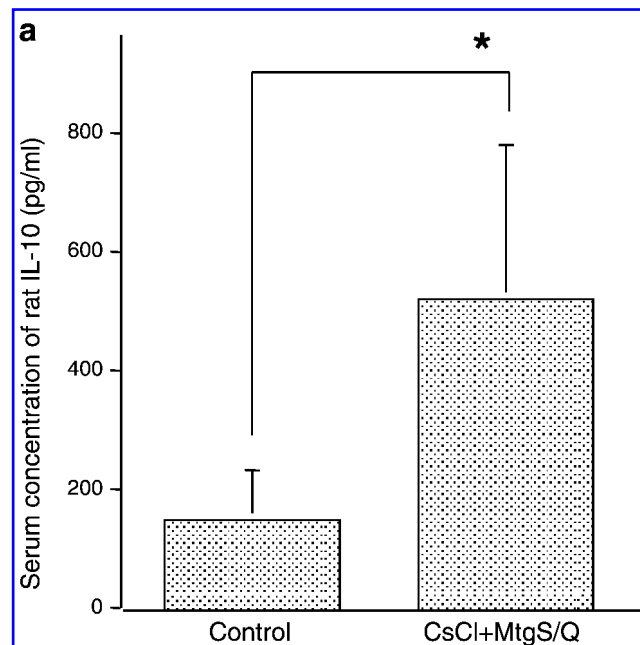


**FIG. 3.** Improved transduction of muscle. (a) Male Wistar rats (3 weeks old) were injected with either CsCl-purified (Control,  $n = 12$ ) or ion-exchange membrane-purified (CsCl + MtgS/Q,  $n = 8$ ) AAV1-IL-10 at  $6 \times 10^{10}$  genome copies per animal via the tibialis anterior muscle. Eight weeks after injection, serum IL-10 concentration was estimated by ELISA. Values represent means  $\pm$  SD. The asterisk indicates  $p < 0.05$ . Histological analysis of the muscle injection site was performed by using ultraviolet-inactivated AAV1-IL-10 vector particles to examine the tissue for signs of toxicity or inflammation. Male *mdx* mice were injected with either (b) PBS or (c) CsCl-purified particles or (d) ion-exchange membrane-purified particles at  $1 \times 10^{11}$  genome copies per animal via the tibialis anterior muscle at 2 weeks of age. Two weeks after injection, the mice were sacrificed and muscle samples were examined by H&E staining. Scale bar, 50  $\mu$ m.

**TABLE 2.** COMPARISON OF RECOMBINANT ADENO-ASSOCIATED VIRUS SEROTYPE 8 OBTAINED FROM TRANSDUCED CELLS AND SUPERNATANTS

Experiment	Yields of rAAV8 in cell pellet or supernatant of transduction culture				Ratio <sup>a</sup>
	Cell pellet		Supernatant		
	Total particles ( $\times 10^{13}$ GC)	Particles per cell ( $\times 10^4$ GC)	Total particles ( $\times 10^{13}$ GC)	Particles per cell ( $\times 10^4$ GC)	
1	3.2	2.2	26.8	18.1	8.4
2	5.7	7.1	32.6	40.8	5.7
3	3.9	1.7	25.2	11.3	6.5
4	3.5	3.2	18.4	17.0	5.3
5	2.2	1.5	47.6	31.3	21.4
6	2.7	1.2	25.6	12.0	9.6
7	7.8	3.6	43.2	19.9	5.6
Average	4.1	2.9	31.3	21.5	7.3

<sup>a</sup>Ratio of particle numbers in supernatant to those in cell pellet.

mice, a mouse model of DMD. The tibialis anterior muscle of control mice injected with PBS showed scarce inflammatory cell infiltration, along with myofibers with central nuclei (Fig. 3b). *mdx* mice injected with CsCl-purified particles demonstrated extensive cellular infiltration with polymorphonuclear and mononuclear cells at the site of injection (Fig. 3c). In contrast, mice injected with the ion-exchange membrane-purified particles revealed manifestation similar to that of the PBS-treated control at 4 weeks of age (Fig. 3d).

#### Scalable vector preparations with dual ion-exchange chromatography

The average recovery of purified recombinant AAV-1 from four different crude virus lysates was 17.4% (data not shown). Although vector yield was dependent on the transgene and construct, recovery up to  $2.0 \times 10^{14}$  vector particles per dual Acrodiscs was achieved. Interestingly, we found that the yield from the supernatant was significantly higher than that from the cell pellet (Table 2). The amount of DNase-resistant particles in the supernatant was 7.3-fold higher than that obtained from the cell pellet ( $n = 7$ ,  $p < 0.001$ ). Furthermore, the ion-exchange protocol using adsorptive membranes was tried to realize effective purification. The bed volume of the adsorptive membrane was only 0.18 ml and this is much less than that of a conventional resin-based column with identical protein capture capacity. Therefore, every step, including capture, wash, and elution procedure, was performed quickly. Consequently, the membrane adsorbers enabled the efficient recovery of rAAV-8 in the 500-ml supernatant of the transduced cells culture (Table 3). To confirm the transduction activity, canine myoblasts were infected with the rAAV8-EGFP produced (Fig. 4). Efficiency of transduction of myoblasts with vectors derived from the culture supernatant was equivalent to that from the cells.

U251MG human glioma cells were transduced with the luciferase-expressing recombinant retroviruses obtained from the various purification procedures (see Supplementary Table 1 at [www.liebertonline.com/hum](http://www.liebertonline.com/hum)). As expected, unlike retroviral vectors pseudotyped with VSV-G protein, retroviral vectors bearing the amphotropic envelope protein could not withstand the shear forces during ultracentrifugation. In contrast, the amphotropic vector was successfully enriched by ion-exchange chromatography without ultracentrifugation. When the transduction efficiency of the enriched sample was compared with that of the initial viral supernatant, the ion-exchange chromatography resulted in good recovery of biologically active amphotropic vectors. Furthermore, a higher recovery rate was observed in transduction with vectors prepared by dual ion-exchange chromatography, relative to transduction with vectors prepared by anion-exchange chromatography alone. The experiment was repeated with similar results.

#### Discussion

In this study, we have described an effective and scalable method for the purification and concentration of rAAV particles as well as amphotropic retroviral vectors. This straightforward method uses cation-exchange followed by anion-exchange chromatography to obtain purified rAAV particles. The AAV vector preparation with dual ion-exchange chromatography allowed higher levels of gene transfer *in vivo* without remarkable signs of toxicity or inflammation. Furthermore, this scalable strategy enabled the recovery of rAAV particles from the transduction culture supernatant, which is normally discarded in the course of the purification procedure. Also, the chromatographic method of concentrating amphotropic retroviral vectors successfully generated serum-free viral stocks with efficient recovery.

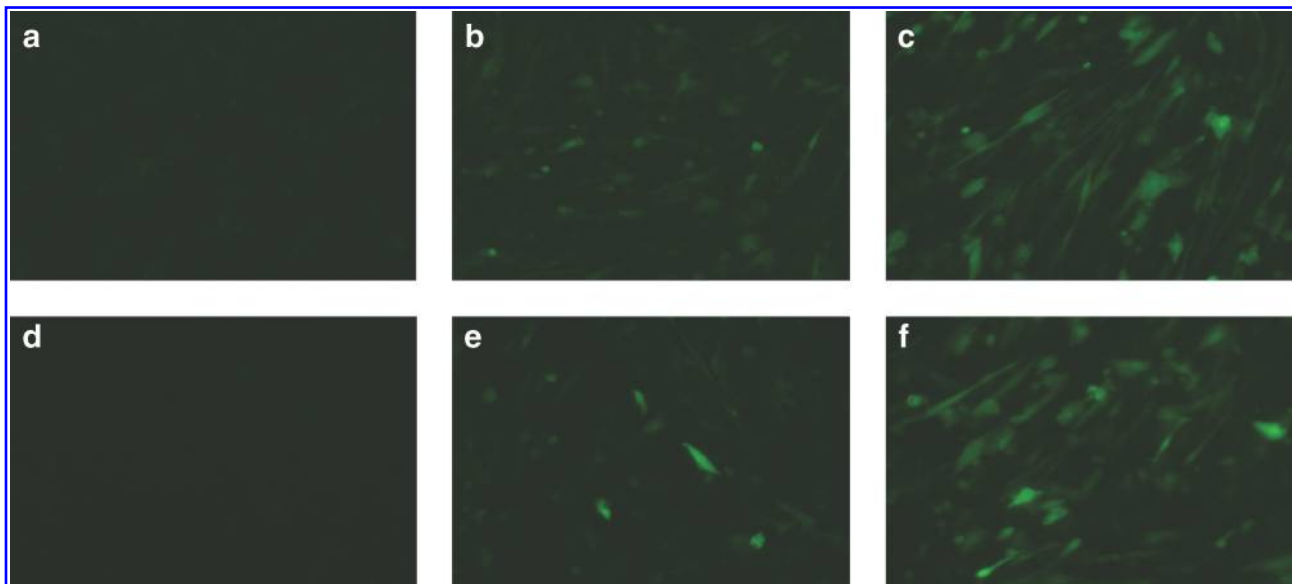


**FIG. 4.** Myoblast transduction with rAAV8 purified from cell pellet or culture supernatant. rAAV8-EGFP was purified from the (a–c) cell pellet or (d–f) supernatant of transduced 293 cell culture. Canine myoblasts were transduced with rAAV8-EGFP at 0 (vehicle; a and d),  $1 \times 10^5$  (b and e), or  $3 \times 10^5$  (c and f) genome copies per cell. Color images available online at [www.liebertonline.com/hum](http://www.liebertonline.com/hum).

TABLE 3. EFFECTIVE RECOVERY OF RECOMBINANT ADENO-ASSOCIATED VIRUS SEROTYPE 8 FROM TRANSDUCED CELL CULTURE SUPERNATANT

Experiment	Particles loaded <sup>a</sup> ( $\times 10^{13}$ GC)	Particles recovered ( $\times 10^{13}$ GC)	Recovery rate <sup>b</sup> (%)
1	7.1	3.2	45
2	8.9	5.8	65
3	8.2	3.0	37

<sup>a</sup>Particles loaded, vector genomes applied to the dual-ion exchange procedure.

<sup>b</sup>Data are from cation exchange at pH 6.5 and anion step at pH 8.0.

Membrane adsorbers provide an attractive alternative to traditional bead-based chromatography columns used to remove impurities in various applications (Phillips *et al.*, 2005). Bead ligands in the packed columns are reached only by long-distance diffusion through pores. Therefore, the purification procedure with resin-based packed-bed chromatography is lengthy, including equilibration, sample application, washing, and elution. In addition, contamination with the distinct vectors will often recur if cost-effective disposable material has not been prepared. In contrast, binding sites in the membrane adsorbers are exposed to the molecules within short diffusion distances. This improved accessibility to the adsorber material makes vector purification processing much easier than with packed-bed chromatography and minimizes the essential bed volume. These characteristics of the disposable ion-exchange membrane save substantial time as well as viral viability. AAV vector purification with membrane adsorbers was effective and allowed higher levels of gene transfer *in vivo* without any signs of toxicity or inflammation. Electron microscopy of the AAV vector stocks obtained revealed highly purified virions with as few as 0.8% empty particles.

IEF is an electrophoresis molecular diagnostic operation that separates protein in a pH gradient according to their *pI*. Because of differences in *pI*, different proteins will focus at different points in the gradient. The *pI* is the specific pH at which the net charge of the protein is zero. The net charge of a virus is the sum of all the negative and positive charges of its amino acid side chains and amino and carboxyl termini along with the packaged DNA in the virion. In this study, we have shown that the *pI* of empty particles was significantly higher than that of packaged virions. Because proteins are positively charged at pH values below their *pI* and negatively charged at pH values above their *pI*, the net positive charge of empty particles would be higher than that of packaged virions at a constant pH below the *pI* of empty particles (see Supplementary Figure 1 at [www.liebertonline.com/hum](http://www.liebertonline.com/hum)). On the other hand, the net negative charge of packaged virions would be stronger than that of empty particles at a constant pH above the *pI* of packaged virions.

Interestingly, we found that the yield from the supernatant was significantly higher than that from the cell pellet. This is probably due to the transduction event in that crumpled transduced cells released a considerable amount of rAAV particles into the culture medium. Therefore, it is practically and theoretically reasonable to use the supernatant of the transduction culture for rAAV production.

However, conventional ion-exchange chromatography, using resin bead-based columns with a huge bed volume size, is a time-consuming procedure. In this respect, the protocol described here, in which small membrane absorbers are used, is an effective and quicker technique.

The method described herein also has several other attractive features. First, purification of rAAV particles with disposable membrane obviates concerns about vector contamination by other infectious agents potentially trapped in an ion-exchange column used for multiple purification procedures. Although a brief centrifugation on CsCl density gradients is used as an initial step, the method reported here does not require high-speed centrifugation over 24 hr, and avoids rounds of isopycnic banding steps to collect vector-containing fractions. In addition, the vector binding and elution properties achieved with the buffers and membrane adsorptive chromatography system produced high-titer vector. Dual ion-exchange chromatography with a brief centrifugation on two-tier CsCl density gradients can effectively avoid destruction of viral particles, which may contribute to the improved transduction efficiency *in vivo* (Kaludov *et al.*, 2002). Future improvements of this method could be made by devising a method to eliminate the initial concentration step by CsCl density gradient. Potentially, the use of detergents, optimized ultrafiltration, or an affinity chromatography could remove a larger percentage of the impurities in the crude lysate so that we may be able to skip the initial two-tier CsCl density gradients.

As a result of our purification procedure, pure stocks with less than 1% empty particles were successfully produced. Although a previous protocol using conventional resin-based anion-exchange chromatography showed reduced contamination by empty particles in the rAAV-1 stock, empty particle contamination of samples was approximately 5% (Urabe *et al.*, 2006). In our study here, elimination of the various impurities might be associated with the better transduction efficiency and minimal inflammatory reaction by dual ion-exchange chromatography compared with CsCl centrifugation. In addition to the effective reduction of empty particles, this protocol also successfully avoided lengthy exposure to CsCl. The conventional method of purification based on rounds of CsCl density centrifugation yields vectors with reduced transduction activity (Gao *et al.*, 2000).

Unlike pseudotyped retroviral vectors bearing the VSV-G protein, retroviral vectors bearing the amphotropic envelope protein cannot withstand the shearing forces of ultracentrifugation. Therefore, the utility of the concentrated amphotropic retroviral vector is limited in the *in vivo* transduction experiment, although it is less toxic compared with the VSV-G-pseudotyped retroviral vector. Besides, suitable transduction medium usually varies with the target cells, although retroviral vector is collected as a vector-containing soup with medium used for 293 cells transduction. However, selection of the medium for 293 cell transfection frequently conflicts with the culture conditions for hematopoietic cells, although it is difficult to replace the suspension medium after harvest of the vector. In contrast, the quick ion-exchange chromatography resulted in good recovery of biologically active recombinant viruses with the amphotropic envelope protein. Elimination of the various impurities might be associated with better recovery of vectors by dual ion-exchange chromatography compared with anion exchange alone.

The production and purification procedures described in this report will expedite gene therapy research by providing a simple, rapid, and effective method for the generation of highly purified vectors. In addition, these procedures may potentially be applied to the production and purification of other vector systems. This closed viral production protocol using disposable membranes is particularly promising, as it easily interfaces with standard FPLC systems as well as syringe pumps. Moreover, the disposable material represents an advantage to meet GMP specifications. This system will provide the basis for further *in vivo* experiments and future clinical investigations.

### Acknowledgments

The authors thank Dr. James M. Wilson for providing chimeric helper plasmids for rAAV1 (p5E18RXCI) and rAAV8 (p5E18-VD2/8). The authors thank Avigen (Alameda, CA) for providing pAAV-LacZ and pAdeno, Dr. M. Onodera (Tsukuba University, Japan) for pGCDN<sub>sap</sub>, Dr. T. Hope (University of Illinois, Chicago, IL) for pBS II SK<sup>+</sup>WPRE-B11, and Dr. J.I. Miyazaki (Osaka University, Japan) for pCAGGS. The authors thank Dr. Mikiharu Yoshida for helpful discussion, and also Ms. Miyoko Mitsu and Ms. Kiyomi Aoki for encouragement and technical support. This study was supported in part by (1) grants from the Ministry of Health, Labor, and Welfare of Japan, (2) Grants-in-Aid for Scientific Research, (3) a grant from the 21st Century COE program, and (4) a "High-Tech Research Center" Project for Private Universities matching fund subsidy, from the Ministry of Education, Culture, Sports, Science, and Technology of Japan.

### Author Disclosure Statement

No competing financial interests exist for all authors.

### References

- Duffy, A.M., O'Doherty, A.M., O'Brien, T., and Strappe, P.M. (2005). Purification of adenovirus and adeno-associated virus: Comparison of novel membrane-based technology to conventional techniques. *Gene Ther.* 12(Suppl. 1), S62–S72.
- Gao, G., Qu, G., Burnham, M.S., Huang, J., Chirmule, N., Joshi, B., Yu, Q.C., Marsh, J.A., Conceicao, C.M., and Wilson, J.M. (2000). Purification of recombinant adeno-associated virus vectors by column chromatography and its performance *in vivo*. *Hum. Gene Ther.* 11, 2079–2091.
- Glimm, H., Flugge, K., Mobest, D., Hofmann, V.M., Postmus, J., Henschler, R., Lange, W., Finke, J., Kiem, H.P., Schulz, G., Rosenthal, F., Mertelsmann, R., and Von Kalle, C. (1998). Efficient serum-free retroviral gene transfer into primitive human hematopoietic progenitor cells by a defined, high-titer, nonconcentrated vector-containing medium. *Hum. Gene Ther.* 9, 771–778.
- Kaludov, N., Handelman, B., and Chiorini, J.A. (2002). Scalable purification of adeno-associated virus type 2, 4, or 5 using ion-exchange chromatography. *Hum. Gene Ther.* 13, 1235–1243.
- Knudsen, H.L., Fahrner, R.L., Xu, Y., Norling, L.A., and Blank, G.S. (2001). Membrane ion-exchange chromatography for process-scale antibody purification. *J. Chromatogr. A* 907, 145–154.
- Merten, O.W., Geny-Fiamma, C., and Douar, A.M. (2005). Current issues in adeno-associated viral vector production. *Gene Ther.* 12(Suppl. 1), S51–S61.
- Okada, T., Shimazaki, K., Nomoto, T., Matsushita, T., Mizukami, H., Urabe, M., Hanazono, Y., Kume, A., Tobita, K., Ozawa, K., and Kawai, N. (2002). Adeno-associated viral vector-mediated gene therapy of ischemia-induced neuronal death. *Methods Enzymol.* 346, 378–393.
- Okada, T., Caplen, N.J., Ramsey, W.J., Onodera, M., Shimazaki, K., Nomoto, T., Ajalli, R., Wildner, O., Morris, J., Kume, A., Hamada, H., Blaese, R.M., and Ozawa, K. (2004). *In situ* generation of pseudotyped retroviral progeny by adenovirus-mediated transduction of tumor cells enhances the killing effect of HSV-tk suicide gene therapy *in vitro* and *in vivo*. *J. Gene Med.* 6, 288–299.
- Okada, T., Nomoto, T., Yoshioka, T., Nonaka-Sarukawa, M., Ito, T., Ogura, T., Iwata-Okada, M., Uchibori, R., Shimazaki, K., Mizukami, H., Kume, A., and Ozawa, K. (2005). Large-scale production of recombinant viruses using a large culture vessel with active gassing. *Hum. Gene Ther.* 16, 1212–1218.
- Ory, D.S., Neugeboren, B.A., and Mulligan, R.C. (1996). A stable human-derived packaging cell line for production of high titer retrovirus/vesicular stomatitis virus G pseudotypes. *Proc. Natl. Acad. Sci. U.S.A.* 93, 11400–11406.
- Phillips, M., Cormier, J., Ferrence, J., Dowd, C., Kiss, R., Lutz, H., and Carter, J. (2005). Performance of a membrane adsorber for trace impurity removal in biotechnology manufacturing. *J. Chromatogr. A* 1078, 74–82.
- Sommer, J.M., Smith, P.H., Parthasarathy, S., Isaacs, J., Vijay, S., Kieran, J., Powell, S.K., McClelland, A., and Wright, J.F. (2003). Quantification of adeno-associated virus particles and empty capsids by optical density measurement. *Mol. Ther.* 7, 122–128.
- Suzuki, A., Obi, K., Urabe, T., Hayakawa, H., Yamada, M., Kaneko, S., Onodera, M., Mizuno, Y., and Mochizuki, H. (2002). Feasibility of *ex vivo* gene therapy for neurological disorders using the new retroviral vector GCDN<sub>sap</sub> packaged in the vesicular stomatitis virus G protein. *J. Neurochem.* 82, 953–960.
- Tamura, K., Tamura, M., Ikenaka, K., Yoshimatsu, T., Miyao, Y., Nanmoku, K., and Shimizu, K. (2001). Eradication of murine brain tumors by direct inoculation of concentrated high titer-recombinant retrovirus harboring the herpes simplex virus thymidine kinase gene. *Gene Ther.* 8, 215–222.
- Urabe, M., Xin, K.Q., Obara, Y., Nakakura, T., Mizukami, H., Kume, A., Okuda, K., and Ozawa, K. (2006). Removal of empty capsids from type 1 adeno-associated virus vector stocks by anion-exchange chromatography potentiates transgene expression. *Mol. Ther.* 13, 823–828.
- Yuasa, K., Sakamoto, M., Miyagoe-Suzuki, Y., Tanouchi, A., Yamamoto, H., Li, J., Chamberlain, J.S., Xiao, X., and Takeda, S. (2002). Adeno-associated virus vector-mediated gene transfer into dystrophin-deficient skeletal muscles evokes enhanced immune response against the transgene product. *Gene Ther.* 9, 1576–1588.

Address correspondence to:

Dr. Takashi Okada  
Department of Molecular Therapy  
National Institute of Neuroscience  
National Center of Neurology and Psychiatry  
4-1-1 Ogawa-Higashi, Kodaira  
Tokyo 187-8502, Japan

E-mail: t-okada@ncnp.go.jp

Received for publication January 13, 2009;  
accepted after revision June 17, 2009.

Published online: August 5, 2009.

**This article has been cited by:**

1. Francesco Destro, Weida Wu, Prasanna Srinivasan, John Joseph, Vivekananda Bal, Caleb Neufeld, Jacqueline M. Wolfrum, Scott R. Manalis, Anthony J. Sinskey, Stacy L. Springs, Paul W. Barone, Richard D. Braatz. 2024. The state of technological advancement to address challenges in the manufacture of rAAV gene therapies. *Biotechnology Advances* **76**, 108433. [[Crossref](#)]
2. Frederik Meierrieks, Alisa Weltken, Karl Pflanz, Andreas Pickl, Benjamin Graf, Michael W. Wolff. 2024. A Novel and Simplified Anion Exchange Flow-Through Polishing Approach for the Separation of Full From Empty Adeno-Associated Virus Capsids. *Biotechnology Journal* **19**:10. . [[Crossref](#)]
3. William S. Kish, John Lightholder, Tamara Zeković, Alex Berrill, Matthew Roach, William B. Wellborn, Eric Vorst. 2024. Removal of empty capsids from high-dose adeno-associated virus 9 gene therapies. *Biotechnology and Bioengineering* **121**:8, 2500-2523. [[Crossref](#)]
4. William R. Keller, Angela Picciano, Kelly Wilson, Jin Xu, Harshit Khata, Michaela Wendeler. 2024. Rational downstream development for adeno-associated virus full/empty capsid separation – A streamlined methodology based on high-throughput screening and mechanistic modeling. *Journal of Chromatography A* **1716**, 464632. [[Crossref](#)]
5. Xuan Lin, Zhiguo Su, Guanghui Ma, Songping Zhang. Separation of bio-particles by ion-exchange chromatography 553-577. [[Crossref](#)]
6. Rimi Miyaoaka, Yuji Tsunekawa, Yae Kurosawa, Takako Sasaki, Azusa Onodera, Kenji Sakamoto, Yuko Kakiuchi, Mikako Wada, Yuko Nitahara-Kasahara, Hiromi Hayashita-Kinoh, Takashi Okada. 2023. Development of a novel purification method for AAV vectors using tangential flow filtration. *Biotechnology and Bioengineering* **120**:11, 3311-3321. [[Crossref](#)]
7. Wenning Chu, Shriarjun Shastry, Eduardo Barbieri, Raphael Prodromou, Paul Greback-Clarke, Will Smith, Brandyn Moore, Ryan Kilgore, Christopher Cummings, Jennifer Pancorbo, Gary Gilleskie, Michael A. Daniele, Stefano Menegatti. 2023. Peptide ligands for the affinity purification of adeno-associated viruses from HEK 293 cell lysates. *Biotechnology and Bioengineering* **120**:8, 2283-2300. [[Crossref](#)]
8. Mikako Wada, Naoya Uchida, Guillermo Posadas-Herrera, Hiromi Hayashita-Kinoh, Yuji Tsunekawa, Yukihiko Hirai, Takashi Okada. 2023. Large-scale purification of functional AAV particles packaging the full genome using short-term ultracentrifugation with a zonal rotor. *Gene Therapy* **30**:7-8, 641-648. [[Crossref](#)]
9. Shaza S. Issa, Alisa A. Shaimardanova, Valeriya V. Solovyeva, Albert A. Rizvanov. 2023. Various AAV Serotypes and Their Applications in Gene Therapy: An Overview. *Cells* **12**:5, 785. [[Crossref](#)]
10. Wenning Chu, Shriarjun Shastry, Eduardo Barbieri, Raphael Prodromou, Paul Greback-Clarke, Will Smith, Brandyn Moore, Ryan Kilgore, Christopher Cummings, Jennifer Pancorbo, Gary Gilleskie, Michael A. Daniele, Stefano Menegatti. Peptide ligands for the affinity purification of adeno-associated viruses from HEK 293 cell lysates **399**, . [[Crossref](#)]
11. Logan Thrasher Collins, Selvarangan Ponnazhagan, David T. Curiel. 2023. Synthetic Biology Design as a Paradigm Shift toward Manufacturing Affordable Adeno-Associated Virus Gene Therapies. *ACS Synthetic Biology* **12**:1, 17-26. [[Crossref](#)]
12. Siddharth Neog, Sachin Kumar, Vishal Trivedi. 2023. Isolation and characterization of Newcastle disease virus from biological fluids using column chromatography. *Biomedical Chromatography* **37**:1. . [[Crossref](#)]
13. Paul Cashen, Katy McLaughlin. Overview of Current Downstream Processing for Modern Viral Vectors 91-123. [[Crossref](#)]
14. Louis Crowley, Jennifer J. Labisch, Maja Leskovec, Mojca Tajnik Sbaizero, Katy Mclaughlin, Piergiuseppe Nestola, Amelie Boulais. Purifying Viral Vectors: A Review of Chromatography Solutions 171-202. [[Crossref](#)]
15. William R. Keller, Angela Picciano, Kelly Wilson, Jin Xu, Harshit Khata, Michaela Wendeler. Rational Downstream Development for Aav Full/Empty Capsid Separation – A Streamlined Methodology Based on High-Throughput Screening and Mechanistic Modeling **18**, . [[Crossref](#)]
16. Spyridon Konstantinidis, Murphy R. Poplyk, Andrew R. Swartz, Richard R. Rustandi, Rachel Thompson, Sheng-Ching Wang. 2022. Application of cation exchange chromatography in bind and elute and flowthrough mode for the purification of enteroviruses. *Journal of Chromatography A* **1676**, 463259. [[Crossref](#)]
17. Lyubava Belova, Konstantin Kochergin-Nikitsky, Anastasia Erofeeva, Alexander Lavrov, Svetlana Smirnikhina. 2022. Approaches to purification and concentration of rAAV vectors for gene therapy. *BioEssays* **44**:6. . [[Crossref](#)]
18. Nicolas Tricaud, Benoit Gautier, Jade Berthelot, Sergio Gonzalez, Gerben Van Hameren. 2022. Traumatic and Diabetic Schwann Cell Demyelination Is Triggered by a Transient Mitochondrial Calcium Release through Voltage Dependent Anion Channel 1. *Biomedicines* **10**:6, 1447. [[Crossref](#)]
19. Adam L. Hejmowski, Kurt Boenning, Julio Huato, Aydin Kavara, Mark Schofield. 2022. Novel anion exchange membrane chromatography method for the separation of empty and full adeno-associated virus. *Biotechnology Journal* **17**:2. . [[Crossref](#)]

20. Yuko Nitahara-Kasahara, Mutsuki Kuraoka, Yuki Oda, Hiromi Hayashita-Kinoh, Shin'ichi Takeda, Takashi Okada. 2021. Enhanced cell survival and therapeutic benefits of IL-10-expressing multipotent mesenchymal stromal cells for muscular dystrophy. *Stem Cell Research & Therapy* **12**:1. . [[Crossref](#)]
21. Elad Lerer, Ziv Oren, Yaron Kafri, Yaakov Adar, Einat Toister, Lilach Cherry, Edith Lupu, Arik Monash, Rona Levy, Eyal Dor, Eyal Epstein, Lilach Levin, Meni Girshengorn, Niva Natan, Ran Zichel, Arik Makovitzki. 2021. Highly Efficient Purification of Recombinant VSV-ΔG-Spike Vaccine against SARS-CoV-2 by Flow-Through Chromatography. *BioTech* **10**:4, 22. [[Crossref](#)]
22. Pavel Marichal-Gallardo, Kathleen Börner, Michael M. Pieler, Vera Sonntag-Buck, Martin Obr, David Bejarano, Michael W. Wolff, Hans-Georg Kräusslich, Udo Reichl, Dirk Grimm. 2021. Single-Use Capture Purification of Adeno-Associated Viral Gene Transfer Vectors by Membrane-Based Steric Exclusion Chromatography. *Human Gene Therapy* **32**:17-18, 959-974. [[Abstract](#)] [[Full Text](#)] [[PDF](#)] [[PDF Plus](#)] [[Supplementary Material](#)]
23. Qing-Hai Xia, Cui-Tao Lu, Meng-Qi Tong, Meng Yue, Rui Chen, De-Li Zhuge, Qing Yao, He-Lin Xu, Ying-Zheng Zhao. 2021. Ganoderma Lucidum Polysaccharides Enhance the Abscopal Effect of Photothermal Therapy in Hepatoma-Bearing Mice Through Immunomodulatory, Anti-Proliferative, Pro-Apoptotic and Anti-Angiogenic. *Frontiers in Pharmacology* **12**. . [[Crossref](#)]
24. Pranav R.H. Joshi, Alice Bernier, Pablo D. Moço, Joseph Schrag, Parminder S. Chahal, Amine Kamen. 2021. Development of a scalable and robust AEX method for enriched rAAV preparations in genome-containing VCs of serotypes 5, 6, 8, and 9. *Molecular Therapy - Methods & Clinical Development* **21**, 341-356. [[Crossref](#)]
25. Santoshkumar L. Khatwani, Anna Pavlova, Zhu Pirot. 2021. Anion-exchange HPLC assay for separation and quantification of empty and full capsids in multiple adeno-associated virus serotypes. *Molecular Therapy - Methods & Clinical Development* **21**, 548-558. [[Crossref](#)]
26. Hiromi Hayashita-Kinoh, Posadas-Herrera Guillermo, Yuko Nitahara-Kasahara, Mutsuki Kuraoka, Hironori Okada, Tomoko Chiyo, Shin'ichi Takeda, Takashi Okada. 2021. Improved transduction of canine X-linked muscular dystrophy with rAAV9-microdystrophin via multipotent MSC pretreatment. *Molecular Therapy - Methods & Clinical Development* **20**, 133-141. [[Crossref](#)]
27. Ryan Dickerson, Christopher Argento, John Pieracci, Meisam Bakhshayeshi. 2021. Separating Empty and Full Recombinant Adeno-Associated Virus Particles Using Isocratic Anion Exchange Chromatography. *Biotechnology Journal* **16**:1. . [[Crossref](#)]
28. Jihad El Andari, Dirk Grimm. 2021. Production, Processing, and Characterization of Synthetic AAV Gene Therapy Vectors. *Biotechnology Journal* **16**:1. . [[Crossref](#)]
29. Keven Lothert, Felix Pagallies, Thomas Feger, Ralf Amann, Michael W. Wolff. 2020. Selection of chromatographic methods for the purification of cell culture-derived Orf virus for its application as a vaccine or viral vector. *Journal of Biotechnology* **323**, 62-72. [[Crossref](#)]
30. Benjamin Adams, Hanne Bak, Andrew D. Tustian. 2020. Moving from the bench towards a large scale, industrial platform process for adeno-associated viral vector purification. *Biotechnology and Bioengineering* **117**:10, 3199-3211. [[Crossref](#)]
31. Nusrat Khan, Shubham Maurya, Sridhar Bammedi, Giridhara R. Jayandharan. 2020. AAV6 Vexosomes Mediate Robust Suicide Gene Delivery in a Murine Model of Hepatocellular Carcinoma. *Molecular Therapy - Methods & Clinical Development* **17**, 497-504. [[Crossref](#)]
32. Daniel Loewe, Hauke Dieken, Tanja A. Grein, Tobias Weidner, Denise Salzig, Peter Czermak. 2020. Opportunities to debottleneck the downstream processing of the oncolytic measles virus. *Critical Reviews in Biotechnology* **40**:2, 247-264. [[Crossref](#)]
33. Liujiang Song, Jacquelyn J. Bower, Matthew L. Hirsch. Preparation and Administration of Adeno-associated Virus Vectors for Corneal Gene Delivery 77-102. [[Crossref](#)]
34. Chunlei Wang, Sri Hari Raju Mulagapati, Zhongying Chen, Jing Du, Xiaohui Zhao, Guoling Xi, Liyan Chen, Thomas Linke, Cuihua Gao, Albert E. Schmelzer, Dengfeng Liu. 2019. Developing an Anion Exchange Chromatography Assay for Determining Empty and Full Capsid Contents in AAV6.2. *Molecular Therapy - Methods & Clinical Development* **15**, 257-263. [[Crossref](#)]
35. Toyokazu Kimura, Beatriz Ferran, Yuko Tsukahara, Qifan Shang, Suveer Desai, Alessandra Fedoce, David Richard Pimentel, Ivan Luptak, Takeshi Adachi, Yasuo Ido, Reiko Matsui, Markus Michael Bachschmid. 2019. Production of adeno-associated virus vectors for in vitro and in vivo applications. *Scientific Reports* **9**:1. . [[Crossref](#)]
36. Mehdi Dehghani, Kilean Lucas, Jonathan Flax, James McGrath, Thomas Gaborski. 2019. Tangential Flow Microfluidics for the Capture and Release of Nanoparticles and Extracellular Vesicles on Conventional and Ultrathin Membranes. *Advanced Materials Technologies* **4**:11. . [[Crossref](#)]
37. Tomono Taro, Hirai Yukihiko, Chono Hideto, Mineno Junichi, Ishii Akiko, Onodera Masafumi, Tamaoka Akira, Okada Takashi. 2019. Infectivity Assessment of Recombinant Adeno-Associated Virus and Wild-Type Adeno-Associated Virus Exposed to Various Diluents and Environmental Conditions. *Human Gene Therapy Methods* **30**:4, 137-143. [[Abstract](#)] [[Full Text](#)] [[PDF](#)] [[PDF Plus](#)] [[Supplementary Material](#)]

38. Mochao Zhao, Melissa Vandersluis, James Stout, Ulrich Haupts, Matthew Sanders, Renaud Jacquemart. 2019. Affinity chromatography for vaccines manufacturing: Finally ready for prime time?. *Vaccine* **37**:36, 5491-5503. [[Crossref](#)]
39. Mehdi Dehghani, Kilean Lucas, Jonathan Flax, James McGrath, Thomas Gaborski. Tangential flow microfluidics for the capture and release of nanoparticles and extracellular vesicles on conventional and ultrathin membranes **96**, . [[Crossref](#)]
40. Kuniko Shimazaki, Takashi Kobari, Keiji Oguro, Hidenori Yokota, Yuko Kasahara, Yoshiya Murashima, Eiju Watanabe, Kensuke Kawai, Takashi Okada. 2019. Hippocampal GAD67 Transduction Using rAAV8 Regulates Epileptogenesis in EL Mice. *Molecular Therapy - Methods & Clinical Development* **13**, 180-186. [[Crossref](#)]
41. Nicolas Tricaud, Benoit Gautier, Gerben Van Hameren, Jade Berthelot, Sergio Gonzalez, Roman Chrast. Schwann cell demyelination is triggered by a transient mitochondrial calcium release through Voltage Dependent Anion Channel 1 **74**, . [[Crossref](#)]
42. S. Ranil Wickramasighe, Namila, Rong Fan, Xianghong Qian. Virus Removal and Virus Purification 69-96. [[Crossref](#)]
43. Daniel Hoffmann, Jasmin Leber, Daniel Loewe, Keven Lothert, Tobias Oppermann, Jan Zitzmann, Tobias Weidner, Denise Salzig, Michael Wolff, Peter Czermak. Purification of New Biologicals Using Membrane-Based Processes 123-150. [[Crossref](#)]
44. Taro Tomono, Yukihiko Hirai, Hironori Okada, Yoshitaka Miyagawa, Kumi Adachi, Shuhei Sakamoto, Yasuhiro Kawano, Hideto Chono, Junichi Mineno, Akiko Ishii, Takashi Shimada, Masafumi Onodera, Akira Tamaoka, Takashi Okada. 2018. Highly Efficient Ultracentrifugation-free Chromatographic Purification of Recombinant AAV Serotype 9. *Molecular Therapy - Methods & Clinical Development* **11**, 180-190. [[Crossref](#)]
45. Yusaku Iwasaki, Mio Sendo, Katsuya Dezaki, Tohru Hira, Takehiro Sato, Masanori Nakata, Chayon Goswami, Ryohei Aoki, Takeshi Arai, Parmila Kumari, Masaki Hayakawa, Chiaki Masuda, Takashi Okada, Hiroshi Hara, Daniel J. Drucker, Yuichiro Yamada, Masaaki Tokuda, Toshihiko Yada. 2018. GLP-1 release and vagal afferent activation mediate the beneficial metabolic and chronotherapeutic effects of D-allulose. *Nature Communications* **9**:1. . [[Crossref](#)]
46. Masashi Fukuoka, Masaki Takahashi, Hiromi Fujita, Tomoko Chiyo, H. Akiko Popiel, Shoko Watanabe, Hirokazu Furuya, Miho Murata, Keiji Wada, Takashi Okada, Yoshitaka Nagai, Hirohiko Hohjoh. 2018. Supplemental Treatment for Huntington's Disease with miR-132 that Is Deficient in Huntington's Disease Brain. *Molecular Therapy - Nucleic Acids* **11**, 79-90. [[Crossref](#)]
47. Bence György, Casey A. Maguire. 2018. Extracellular vesicles: nature's nanoparticles for improving gene transfer with adeno-associated virus vectors. *WIREs Nanomedicine and Nanobiotechnology* **10**:3. . [[Crossref](#)]
48. Kuniyuki Endo, Shinsuke Ishigaki, Yoshito Masamizu, Yusuke Fujioka, Akiya Watakabe, Tetsuo Yamamori, Nobuhiko Hatanaka, Atsushi Nambu, Haruo Okado, Masahisa Katsuno, Hirohisa Watanabe, Masanori Matsuzaki, Gen Sobue. 2018. Silencing of FUS in the common marmoset (*Callithrix jacchus*) brain via stereotaxic injection of an adeno-associated virus encoding shRNA. *Neuroscience Research* **130**, 56-64. [[Crossref](#)]
49. Magalie Penaud-Budloo, Achille François, Nathalie Clément, Eduard Ayuso. 2018. Pharmacology of Recombinant Adeno-associated Virus Production. *Molecular Therapy - Methods & Clinical Development* **8**, 166-180. [[Crossref](#)]
50. Schnödt Maria, Büning Hildegard. 2017. Improving the Quality of Adeno-Associated Viral Vector Preparations: The Challenge of Product-Related Impurities. *Human Gene Therapy Methods* **28**:3, 101-108. [[Abstract](#)] [[Full Text](#)] [[PDF](#)] [[PDF Plus](#)]
51. Marc-André Robert, Parminder S. Chahal, Alexandre Audy, Amine Kamen, Rénaud Gilbert, Bruno Gaillet. 2017. Manufacturing of recombinant adeno-associated viruses using mammalian expression platforms. *Biotechnology Journal* **12**:3. . [[Crossref](#)]
52. Barbara Leuchs, Mandy Roscher, Marcus Müller, Kathrin Kürschner, Jean Rommelaere. 2016. Standardized large-scale H-1PV production process with efficient quality and quantity monitoring. *Journal of Virological Methods* **229**, 48-59. [[Crossref](#)]
53. Sergio Gonzalez, Jade Berthelot, Jennifer Jiner, Claire Perrin-Tricaud, Ruani Fernando, Roman Chrast, Guy Lenaers, Nicolas Tricaud. 2016. Blocking mitochondrial calcium release in Schwann cells prevents demyelinating neuropathies. *Journal of Clinical Investigation* **126**:3, 1023-1038. [[Crossref](#)]
54. Benskey Matthew J., Sandoval Ivette M., Manfredsson Fredric P. 2016. Continuous Collection of Adeno-Associated Virus from Producer Cell Medium Significantly Increases Total Viral Yield. *Human Gene Therapy Methods* **27**:1, 32-45. [[Abstract](#)] [[Full Text](#)] [[PDF](#)] [[PDF Plus](#)] [[Supplementary Material](#)]
55. Taro Tomono, Yukihiko Hirai, Hironori Okada, Kumi Adachi, Akiko Ishii, Takashi Shimada, Masafumi Onodera, Akira Tamaoka, Takashi Okada. 2016. Ultracentrifugation-free chromatography-mediated large-scale purification of recombinant adeno-associated virus serotype 1 (rAAV1). *Molecular Therapy - Methods & Clinical Development* **3**, 15058. [[Crossref](#)]
56. Bryan A Piras, Jason E Drury, Christopher L Morton, Yunyu Spence, Timothy D Lockey, Amit C Nathwani, Andrew M Davidoff, Michael M Meagher. 2016. Distribution of AAV8 particles in cell lysates and culture media changes with time and is dependent on the recombinant vector. *Molecular Therapy - Methods & Clinical Development* **3**, 16015. [[Crossref](#)]

57. Nathalie Clément, Joshua C Grieger. 2016. Manufacturing of recombinant adeno-associated viral vectors for clinical trials. *Molecular Therapy - Methods & Clinical Development* 3, 16002. [[Crossref](#)]
58. Pierre-Olivier Buclez, Gabriella Dias Florencio, Karima Relizani, Cyriaque Beley, Luis Garcia, Rachid Benchaouir. 2016. Rapid, scalable, and low-cost purification of recombinant adeno-associated virus produced by baculovirus expression vector system. *Molecular Therapy - Methods & Clinical Development* 3, 16035. [[Crossref](#)]
59. Tsuyoshi Udagawa, Yusuke Fujioka, Motoki Tanaka, Daiyu Honda, Satoshi Yokoi, Yuichi Riku, Daisuke Ibi, Taku Nagai, Kiyofumi Yamada, Hirohisa Watanabe, Masahisa Katsuno, Toshifumi Inada, Kinji Ohno, Masahiro Sokabe, Haruo Okado, Shinsuke Ishigaki, Gen Sobue. 2015. FUS regulates AMPA receptor function and FTLD/ALS-associated behaviour via GluA1 mRNA stabilization. *Nature Communications* 6:1. . [[Crossref](#)]
60. Yoshihisa Ohtsuka, Motoi Kanagawa, Chih-Chieh Yu, Chiyomi Ito, Tomoko Chiyo, Kazuhiro Kobayashi, Takashi Okada, Shin'ichi Takeda, Tatsushi Toda. 2015. Fukutin is prerequisite to ameliorate muscular dystrophic phenotype by myofiber-selective LARGE expression. *Scientific Reports* 5:1. . [[Crossref](#)]
61. Sergio Gonzalez, Ruani Fernando, Jade Berthelot, Claire Perrin-Tricaud, Emmanuelle Sarzi, Roman Chrast, Guy Lenaers, Nicolas Tricaud. 2015. In vivo time-lapse imaging of mitochondria in healthy and diseased peripheral myelin sheath. *Mitochondrion* 23, 32-41. [[Crossref](#)]
62. Maxime Ferrand, Sylvie Da Rocha, Guillaume Corre, Anne Galy, Florence Boisgerault. 2015. Serotype-specific Binding Properties and Nanoparticle Characteristics Contribute to the Immunogenicity of rAAV1 Vectors. *Molecular Therapy* 23:6, 1022-1033. [[Crossref](#)]
63. Hiromi Hayashita-Kinoh, Naoko Yugeta, Hironori Okada, Yuko Nitahara-Kasahara, Tomoko Chiyo, Takashi Okada, Shin'ichi Takeda. 2015. Intra-Amniotic rAAV-Mediated Microdystrophin Gene Transfer Improves Canine X-Linked Muscular Dystrophy and May Induce Immune Tolerance. *Molecular Therapy* 23:4, 627-637. [[Crossref](#)]
64. Adam S. Davis, Thais Federici, William C. Ray, Nicholas M. Boulis, Deirdre O'Connor, K. Reed Clark, Jeffrey S. Bartlett. 2015. Rational Design and Engineering of a Modified Adeno-Associated Virus (AAV1)-Based Vector System for Enhanced Retrograde Gene Delivery. *Neurosurgery* 76:2, 216-225. [[Crossref](#)]
65. Gabriella Dias Florencio, Guillaume Precigout, Cyriaque Beley, Pierre-Olivier Buclez, Luis Garcia, Rachid Benchaouir. 2015. Simple downstream process based on detergent treatment improves yield and in vivo transduction efficacy of adeno-associated virus vectors. *Molecular Therapy - Methods & Clinical Development* 2, 15024. [[Crossref](#)]
66. Riichiro Hira, Fuki Ohkubo, Yoshito Masamizu, Masamichi Ohkura, Junichi Nakai, Takashi Okada, Masanori Matsuzaki. 2014. Reward-timing-dependent bidirectional modulation of cortical microcircuits during optical single-neuron operant conditioning. *Nature Communications* 5:1. . [[Crossref](#)]
67. Satkunanathan Stifani, Wheeler Jun, Thorpe Robin, Zhao Yuan. 2014. Establishment of a Novel Cell Line for the Enhanced Production of Recombinant Adeno-Associated Virus Vectors for Gene Therapy. *Human Gene Therapy* 25:11, 929-941. [[Abstract](#)] [[Full Text](#)] [[PDF](#)] [[PDF Plus](#)] [[Supplementary Material](#)]
68. Sumimasa Arimura, Takashi Okada, Tohru Tezuka, Tomoko Chiyo, Yuko Kasahara, Toshiro Yoshimura, Masakatsu Motomura, Nobuaki Yoshida, David Beeson, Shin'ichi Takeda, Yuji Yamanashi. 2014. DOK7 gene therapy benefits mouse models of diseases characterized by defects in the neuromuscular junction. *Science* 345:6203, 1505-1508. [[Crossref](#)]
69. Yoshito Masamizu, Yasuhiro R Tanaka, Yasuyo H Tanaka, Riichiro Hira, Fuki Ohkubo, Kazuo Kitamura, Yoshikazu Isomura, Takashi Okada, Masanori Matsuzaki. 2014. Two distinct layer-specific dynamics of cortical ensembles during learning of a motor task. *Nature Neuroscience* 17:7, 987-994. [[Crossref](#)]
70. Otto-Wilhelm Merten, Matthias Schweizer, Parminder Chahal, Amine A Kamen. 2014. Manufacturing of viral vectors for gene therapy: part I. Upstream processing. *Pharmaceutical Bioprocessing* 2:2, 183-203. [[Crossref](#)]
71. Jerome Denard, Christine Jenny, Véronique Blouin, Philippe Moullier, Fedor Svinartchouk. 2014. Different protein composition and functional properties of adeno-associated virus-6 vector manufactured from the culture medium and cell lysates. *Molecular Therapy - Methods & Clinical Development* 1, 14031. [[Crossref](#)]
72. Mark Potter, Bridget Lins, Mario Mietzsch, Regine Heilbronn, Kim Van Vliet, Paul Chipman, Mavis Agbandje-McKenna, Brian D Cleaver, Nathalie Clément, Barry J Byrne, Sergei Zolotukhin. 2014. A simplified purification protocol for recombinant adeno-associated virus vectors. *Molecular Therapy - Methods & Clinical Development* 1, 14034. [[Crossref](#)]
73. Doria Monica, Ferrara Antonella, Auricchio Alberto. 2013. AAV2/8 Vectors Purified from Culture Medium with a Simple and Rapid Protocol Transduce Murine Liver, Muscle, and Retina Efficiently. *Human Gene Therapy Methods* 24:6, 392-398. [[Abstract](#)] [[Full Text](#)] [[PDF](#)] [[PDF Plus](#)]
74. Valerie Orr, Luyang Zhong, Murray Moo-Young, C. Perry Chou. 2013. Recent advances in bioprocessing application of membrane chromatography. *Biotechnology Advances* 31:4, 450-465. [[Crossref](#)]

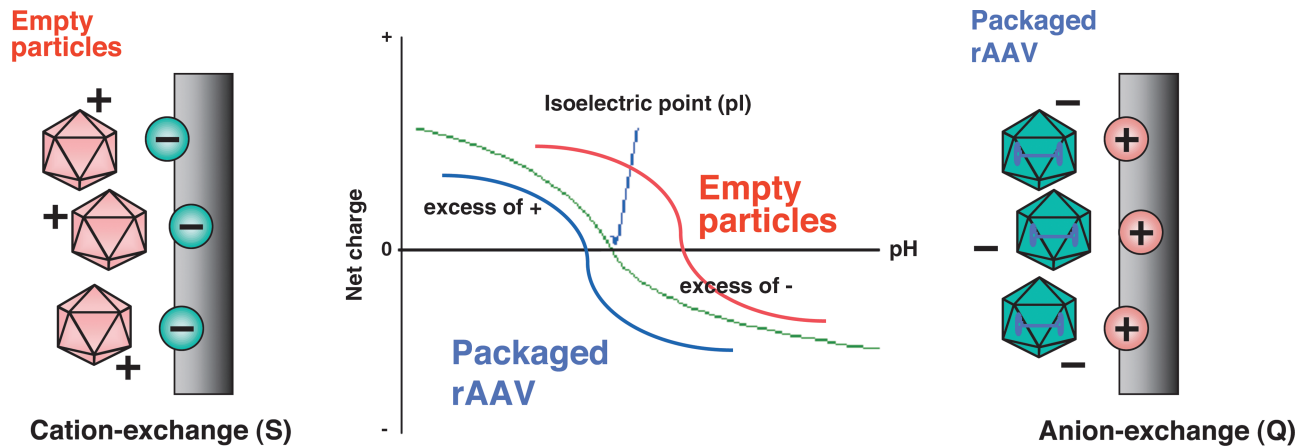
75. Takashi Okada, Shin'ichi Takeda. 2013. Current Challenges and Future Directions in Recombinant AAV-Mediated Gene Therapy of Duchenne Muscular Dystrophy. *Pharmaceuticals* 6:7, 813-836. [[Crossref](#)]
76. Balasubramanian Venkatakrishnan, Joseph Yarbrough, John Domsic, Antonette Bennett, Brian Bothner, Olga G. Kozyreva, R. Jude Samulski, Nicholas Muzyczka, Robert McKenna, Mavis Agbandje-McKenna. 2013. Structure and Dynamics of Adeno-Associated Virus Serotype 1 VP1-Unique N-Terminal Domain and Its Role in Capsid Trafficking. *Journal of Virology* 87:9, 4974-4984. [[Crossref](#)]
77. Hironori Okada, Hidetoshi Ishibashi, Hiromi Hayashita-Kinoh, Tomoko Chiyo, Yuko Nitahara-Kasahara, Yukihiko Baba, Sumiko Watanabe, Shin'ichi Takeda, Takashi Okada. 2013. Robust Long-term Transduction of Common Marmoset Neuromuscular Tissue With rAAV1 and rAAV9. *Molecular Therapy - Nucleic Acids* 2, e95. [[Crossref](#)]
78. Yukihiko Baba, Shinya Satoh, Makoto Otsu, Erika Sasaki, Takashi Okada, Sumiko Watanabe. 2012. In vitro cell subtype-specific transduction of adeno-associated virus in mouse and marmoset retinal explant culture. *Biochimie* 94:12, 2716-2722. [[Crossref](#)]
79. Mikako Ito, Yumi Suzuki, Takashi Okada, Takayasu Fukudome, Toshiro Yoshimura, Akio Masuda, Shin'ichi Takeda, Eric Krejci, Kinji Ohno. 2012. Protein-anchoring Strategy for Delivering Acetylcholinesterase to the Neuromuscular Junction. *Molecular Therapy* 20:7, 1384-1392. [[Crossref](#)]
80. Martin Lock, Mauricio R. Alvira, James M. Wilson. 2012. Analysis of Particle Content of Recombinant Adeno-Associated Virus Serotype 8 Vectors by Ion-Exchange Chromatography. *Human Gene Therapy Methods* 23:1, 56-64. [[Abstract](#)] [[Full Text](#)] [[PDF](#)] [[PDF Plus](#)]
81. Lijun Wang, Véronique Blouin, Nicole Brument, Mahajoub Bello-Roufai, Achille Francois. Production and Purification of Recombinant Adeno-Associated Vectors 361-404. [[Crossref](#)]
82. Kleopatra Rapti, Roger J. Hajjar, Thomas Weber. Novel Approaches to Deliver Molecular Therapeutics in Cardiac Disease Using Adeno-Associated Virus Vectors 391-458. [[Crossref](#)]
83. Yuko Nitahara-Kasahara, Hiromi Hayashita-Kinoh, Sachiko Ohshima-Hosoyama, Hironori Okada, Michiko Wada-Maeda, Akinori Nakamura, Takashi Okada, Shin'ichi Takeda. 2012. Long-term Engraftment of Multipotent Mesenchymal Stromal Cells That Differentiate to Form Myogenic Cells in Dogs With Duchenne Muscular Dystrophy. *Molecular Therapy* 20:1, 168-177. [[Crossref](#)]
84. Tiago Vicente, José P.B. Mota, Cristina Peixoto, Paula M. Alves, Manuel J.T. Carrondo. 2011. Rational design and optimization of downstream processes of virus particles for biopharmaceutical applications: Current advances. *Biotechnology Advances* 29:6, 869-878. [[Crossref](#)]
85. Y. Masamizu, T. Okada, K. Kawasaki, H. Ishibashi, S. Yuasa, S. Takeda, I. Hasegawa, K. Nakahara. 2011. Local and retrograde gene transfer into primate neuronal pathways via adeno-associated virus serotype 8 and 9. *Neuroscience* 193, 249-258. [[Crossref](#)]
86. Michael W Wolf, Udo Reichl. 2011. Downstream processing of cell culture-derived virus particles. *Expert Review of Vaccines* 10:10, 1451-1475. [[Crossref](#)]
87. Taeyoung Koo, Takashi Okada, Takis Athanasopoulos, Helen Foster, Shin'ichi Takeda, George Dickson. 2011. Long-term functional adeno-associated virus-microdystrophin expression in the dystrophic CXMDj dog. *The Journal of Gene Medicine* 13:9, 497-506. [[Crossref](#)]
88. J-H Shin, Y Nitahara-Kasahara, H Hayashita-Kinoh, S Ohshima-Hosoyama, K Kinoshita, T Chiyo, H Okada, T Okada, S Takeda. 2011. Improvement of cardiac fibrosis in dystrophic mice by rAAV9-mediated microdystrophin transduction. *Gene Therapy* 18:9, 910-919. [[Crossref](#)]
89. Tiago Vicente, René Fáber, Paula M. Alves, Manuel J.T. Carrondo, José P.B. Mota. 2011. Impact of ligand density on the optimization of ion-exchange membrane chromatography for viral vector purification. *Biotechnology and Bioengineering* 108:6, 1347-1359. [[Crossref](#)]
90. James A. Allay, Susan Sleep, Scott Long, David M. Tillman, Rob Clark, Gael Carney, Paolo Fagone, Jenny H. McIntosh, Arthur W. Nienhuis, Andrew M. Davidoff, Amit C. Nathwani, John T. Gray. 2011. Good Manufacturing Practice Production of Self-Complementary Serotype 8 Adeno-Associated Viral Vector for a Hemophilia B Clinical Trial. *Human Gene Therapy* 22:5, 595-604. [[Abstract](#)] [[Full Text](#)] [[PDF](#)] [[PDF Plus](#)]
91. María Mercedes Segura, Amine A. Kamen, Alain Garnier. Overview of Current Scalable Methods for Purification of Viral Vectors 89-116. [[Crossref](#)]
92. Martin Lock, Mauricio Alvira, Luk H. Vandenberghe, Arabinda Samanta, Jaan Toelen, Zeger Debyser, James M. Wilson. 2010. Rapid, Simple, and Versatile Manufacturing of Recombinant Adeno-Associated Viral Vectors at Scale. *Human Gene Therapy* 21:10, 1259-1271. [[Abstract](#)] [[Full Text](#)] [[PDF](#)] [[PDF Plus](#)]

93. Luk H. Vandenberghe, Ru Xiao, Martin Lock, Jianping Lin, Michael Korn, James M. Wilson. 2010. Efficient Serotype-Dependent Release of Functional Vector into the Culture Medium During Adeno-Associated Virus Manufacturing. *Human Gene Therapy* **21**:10, 1251-1257. [[Abstract](#)] [[Full Text](#)] [[PDF](#)] [[PDF Plus](#)]
94. TAKASHI OKADA, SHIN'ICHI TAKEDA. 2010. ADVANCES IN MOLECULAR THERAPY RESEARCH ON DYSTROPHIN-DEFICIENT MUSCULAR DYSTROPHY. *Gene Therapy and Regulation* **05**:01, 113-123. [[Crossref](#)]
95. Yoshito Masamizu, Takashi Okada, Hidetoshi Ishibashi, Shin'ichi Takeda, Shigeki Yuasa, Kiyoshi Nakahara. 2010. Efficient gene transfer into neurons in monkey brain by adeno-associated virus 8. *NeuroReport* **21**:6, 447-451. [[Crossref](#)]
96. Colin R. Parrish. Structures and Functions of Parvovirus Capsids and the Process of Cell Infection 149-176. [[Crossref](#)]

SUPPLEMENTARY TABLE 1. EFFICIENT CONCENTRATION AND PURIFICATION OF THE AMPHOTROPIC RETROVIRUS VECTOR

	Centrifugation		Ion-exchange	
	(50k g×2 hr)	(6k g×16 hr)	(S + Q)	(Q)
env	1.3	4.4	43.0	24.3
VSV-G	45.9	52.2	50.9	22.0

The amphotropic or VSV-G-pseudotyped vector was centrifuged at 50,000 g for 2 h or 6000 g for 16 h at 4°C. Alternatively, the sample was concentrated and purified with a dual ion-exchange chromatography procedure (S+Q) or an anion-exchange procedure (Q). U251MG cells were transduced with the luciferase expressing recombinant retroviruses to evaluate the effectiveness of the various purification procedures. At 96 h after transduction, luciferase expression in the cells was analyzed. Transgene expression identified as relative light unit was analyzed to calculate recovery rate of the biologically active vector (%). Recovery rates for the amphotropic-enveloped (env) or VSV-G-pseudotyped (VSV-G) vector were compared to the viral supernatant before enrichment.



SUPPLEMENTARY FIG. 1. The pI is the specific pH at which the net charge of the protein is zero. The net charge of a virus is the sum of all the negative and positive charges of its amino acid side chains and amino- and carboxyl-termini along with the packaged DNA in the virion. We showed that pI of empty particles is higher than that of packaged virions. Since proteins are positively charged at pH values below their pI and negatively charged at pH values above their pI, the net positive charge of empty particles would be higher than that of packaged rAAV particles at a constant pH below the pI of empty particles. On the other hand, the net negative charge of packaged virions would be stronger than that of empty particles at a constant pH above the pI of packaged virions.